The Astrophysical Journal Letters, 769:L20 (5pp), 2013 June 1 doi:10.1088/2041-8205/769/2/L20

DIRECT DIAGNOSTICS OF FORMING MASSIVE STARS: STELLAR PULSATION AND PERIODIC VARIABILITY OF MASER SOURCES

Kohei Inayoshi[1], Koichiro Sugiyama[2], Takashi Hosokawa[3], Kazuhito Motogi[4], and Kei E. I. Tanaka[1,5]
[1] Department of Physics, Graduate School of Science, Kyoto University, Kyoto 606-8502, Japan; inayoshi@tap.scphys.kyoto-u.ac.jp
[2] Graduate School of Science and Engineering, Yamaguchi University, 1677-1 Yoshida, Yamaguchi, Yamaguchi 753-8512, Japan; koichiro@yamaguchi-u.ac.jp
[3] Department of Physics, University of Tokyo, Tokyo 113-0033, Japan; takashi.hosokawa@phys.s.u-tokyo.ac.jp
[4] The Research Institute for Time Studies, Yamaguchi University, Yoshida 1677-1, Yamaguchi, Yamaguchi 753-8511, Japan
[5] Astronomical Institute, Tohoku University, Miyagi 980-8578, Japan
Received 2013 March 4; accepted 2013 April 18; published 2013 May 9

ABSTRACT

The 6.7 GHz methanol maser emission, a tracer of forming massive stars, sometimes shows enigmatic periodic flux variations over several 10–100 days. In this Letter, we propose that these periodic variations could be explained by the pulsation of massive protostars growing under rapid mass accretion with rates of $\dot{M}_* \gtrsim 10^{-3}\,M_\odot\,\mathrm{yr}^{-1}$. Our stellar evolution calculations predict that the massive protostars have very large radii exceeding 100 $R_\odot$ at maximum, and here we study the pulsational stability of such bloated protostars by way of the linear stability analysis. We show that the protostar becomes pulsationally unstable with various periods of several 10–100 days depending on different accretion rates. With the fact that the stellar luminosity when the star is pulsationally unstable also depends on the accretion rate, we derive the period–luminosity relation $\log(L/L_\odot) = 4.62 + 0.98\log(P/100\,\mathrm{days})$, which is testable with future observations. Our models further show that the radius and mass of the pulsating massive protostar should also depend on the period. It would be possible to infer such protostellar properties and the accretion rate with the observed period. Measuring the maser periods enables a direct diagnosis of the structure of accreting massive protostars, which are deeply embedded in dense gas and are inaccessible with other observations.

Key words: masers – stars: massive – stars: oscillations

Online-only material: color figures

1. INTRODUCTION

Massive stars have significant impact on the interstellar medium through various feedback processes such as supernova explosions, stellar winds, and ultraviolet radiation. These feedback processes would also be important for shaping the stellar initial mass function because stars are mostly formed in clusters including massive stars (e.g., Lada & Lada 2003). However, our understanding of the massive star formation is still limited by observational difficulties, one of which arises from the fact that forming massive stars are deeply embedded in obscuring dense gas.

Observing maser emission is one of the possible methods to see the vicinity ($<10^3$ AU) of forming massive stars because of the high brightness. It is known that the 6.7 GHz methanol maser emission can be thought to often be associated with circumstellar disks around forming massive stars (e.g., Norris et al. 1993; Bartkiewicz et al. 2009; Sanna et al. 2010). Some of the methanol masers show periodic flux variations over $\gtrsim$10 days (e.g., Goedhart et al. 2004, 2009). Since the 6.7 GHz methanol masers are radiatively pumped by infrared emission of warm dusts ($\sim$150 K; Cragg et al. 2005), the periodicity could reflect the luminosity variation of nearby forming massive stars or accretion disks.

Several authors have proposed different explanations for these periodic flux variations, e.g., colliding-wind binary (van der Walt 2011), and periodic accretion onto binary systems (Araya et al. 2010). However, these binary-based models do not explain why the periodic variations shorter than 10 days have not yet been found despite the fact that a number of OB star eclipsing binaries have periods of $<$10 days (Harries et al. 2003; Hilditch et al. 2005)

In this Letter, we propose an alternative picture that the periodic variability of the maser emission can be due to the pulsation of protostars growing via rapid mass accretion with $\dot{M}_* \gtrsim 10^{-3}\,M_\odot\,\mathrm{yr}^{-1}$, which is expected in massive star formation (e.g., Osorio et al. 1999; McKee & Tan 2003; Zhang et al. 2005; Beltrán et al. 2006; Krumholz et al. 2009). Our previous work shows that, by numerically modeling the stellar evolution, the massive protostar should have a large radius exceeding 100 $R_\odot$ with such a high accretion rate (Hosokawa & Omukai 2009; Hosokawa et al. 2010, hereafter HO09 and HYO10, respectively). We here examine the pulsational stability of the bloated massive protostars with the linear stability analysis, and show that the observed periodicity of $\sim$10–100 days can be well explained with the stellar pulsation. Our models predict that, with the observed period of the pulsation, we could infer the radius, mass, and luminosity of the protostars as well as the accretion rate onto the protostar. Measuring the maser periods would thus make a direct diagnosis of the central small-scale ($\lesssim$a few AU) structure of forming massive stars, which is beyond observations in the optical and infrared bands.

2. PULSATIONAL INSTABILITY OF ACCRETING MASSIVE STARS

We study the pulsational stability of massive protostars growing at constant accretion rates of $\dot{M}_* \geqslant 10^{-4}\,M_\odot\,\mathrm{yr}^{-1}$. We here adopt the protostellar models with spherical accretion taken from HO09. In Section 3, we will discuss that the effects of the accretion geometry (disk accretion) do not change the qualitative results from the spherical accretion case. Figure 1 shows the evolution of the stellar radius as the stellar mass increases with different accretion rates. The outline of the

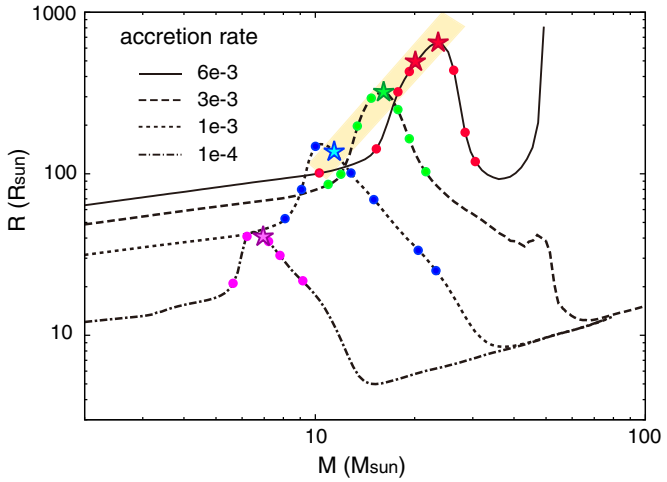

Figure 1. Evolution of the protostellar radius with various accretion rates $\dot{M}_* = 10^{-4}$, 10^{-3}, 3×10^{-3}, and $6 \times 10^{-3}\ M_\odot\ \mathrm{yr}^{-1}$ (taken from HO09). The symbols indicate the stellar models for which we conduct the linear stability analysis. The circles and stars represent the pulsationally stable and unstable models, respectively. The shaded layer denotes the *instability strip* where the protostar becomes unstable.

(A color version of this figure is available in the online journal.)

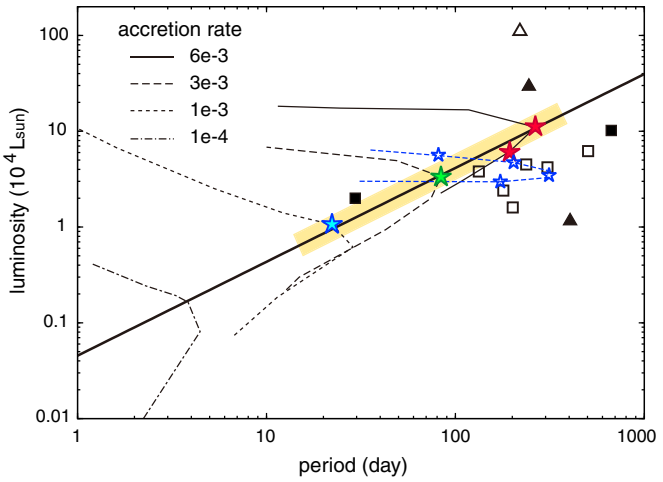

Figure 2. Period–luminosity (P–L) relation of forming massive protostars. The thin black (blue) curves show the evolutionary tracks with the spherical (disk) accretion at the rates of $\dot{M}_* = 10^{-4}$, 10^{-3}, 3×10^{-3}, and $6 \times 10^{-3}\ M_\odot\ \mathrm{yr}^{-1}$. The star symbols on the tracks denote the pulsationally unstable models. The eigen frequencies are plotted for the stable stellar models. The shaded layer shows the instability strip as in Figure 1. The solid line represents the P–L relation given by Equation (1), which fits the unstable models. The filled and open symbols represent the observed sources whose distances are measured with the trigonometric parallax and kinematics. The triangles indicate that the sources are associated with ultra/hypercompact H II regions (Walsh et al. 1998; Reid et al. 2009a; Urquhart et al. 2007).

(A color version of this figure is available in the online journal.)

evolution is briefly summarized as follows (see HO09 for details). Initially, the stellar radius gradually increases with increasing stellar mass. After this stage, e.g., $M_* \gtrsim 10\,M_\odot$ for $\dot{M}_* = 10^{-3}\ M_\odot\ \mathrm{yr}^{-1}$, the protostar contracts by losing its energy via radiation (Kelvin–Helmholtz or KH contraction). The stellar central temperature increases during this contraction stage and finally reaches 10^7 K. The hydrogen burning is ignited and the protostar reaches the zero-age main sequence (ZAMS; except with $6 \times 10^{-3}\ M_\odot\ \mathrm{yr}^{-1}$). After this point, e.g., $M_* \simeq 40\,M_\odot$ for $\dot{M}_* = 10^{-3}\ M_\odot\ \mathrm{yr}^{-1}$, the stellar radius increases again as the stellar mass increases. We here note that the maximum stellar radius during this evolution is larger with a higher accretion rate. This is because the accreting gas has a higher specific entropy with more rapid mass accretion, which leads to a higher average entropy in the stellar interior (also see HO09). As a result, the maximum stellar radius exceeds $100\,R_\odot$ with high accretion rates, $\dot{M}_* \gtrsim 10^{-3}\ M_\odot\ \mathrm{yr}^{-1}$.

We apply the linear stability analysis to the above protostellar models (see, e.g., Cox 1980; Unno et al. 1989; Inayoshi et al. 2013 for details). We here consider radial (spherical) perturbations with the time dependence of $e^{i\sigma t}$, where $\sigma = \sigma_\mathrm{R} + i\sigma_\mathrm{I}$ is the eigen frequency, σ_R is the frequency of the pulsation, and $|\sigma_\mathrm{I}|$ is the growth or damping rate of the perturbation. The protostar is pulsationally stable (unstable) with the positive (negative) σ_I. If unstable, the perturbation grows until it reaches the nonlinear regime, where the pulsation energy is dissipated by shock waves near the stellar surface. The dissipated energy is partly converted into the kinetic energy of periodic outflows (e.g., Appenzeller 1970; Yoon & Cantiello 2010).

The symbols in Figure 1 represent the stellar models for which we conduct the linear stability analysis. Our calculations show that the protostar becomes pulsationally unstable only when the stellar radius expands maximally at a given accretion rate. This instability is caused by the κ mechanism in the He^+ ionization layer, where the radiative energy flux is blocked and converted into the pulsation energy (e.g., Cox 1980; Unno et al. 1989). In the KH contraction stage, the stellar surface temperature increases and the He^+ ionization layer disappears. The protostar is consequently stabilized and the pulsation ceases. Although the protostar would also be unstable with lower accretion rates ($\lesssim 10^{-3}\ M_\odot\ \mathrm{yr}^{-1}$), the growth time is much longer than the duration for which the star is in the instability strip ($\sigma_\mathrm{I}^{-1} \gg M_*/\dot{M}_* \sim 10^4$ yr). The perturbation does not grow enough to cause the stellar pulsation in this case. The instability strip thus does not extend for $M_* \lesssim 10\,M_\odot$, where the star becomes unstable with the lower accretion rate (see Figure 1).

3. PERIOD–LUMINOSITY RELATION

Figure 2 shows the evolution of the pulsation period and stellar luminosity in the examined cases. In each case, the stellar luminosity increases monotonically as the stellar mass increases. The pulsation period increases with the stellar mass in the early expansion phase, and decreases in the later KH contraction phase. The protostar becomes pulsationally unstable around the turning point of the period, which corresponds to that of the stellar radius as seen in Figure 1.

Figure 2 also presents the observed sources with periodic flux variations in the 6.7 GHz methanol masers, whose parameters are summarized in Table 1. The luminosities of these sources are estimated with the far-infrared data of *Infrared Astronomical Satellite* (*IRAS*) following Casoli et al. (1986) and Guzmán et al. (2012). We see that the pulsation periods of the unstable models are several 10–100 days, the same order of the observed periods of the maser sources. Although the pulsation period is shorter than 10 days with low accretion rates $\dot{M}_* \lesssim 10^{-3}\ M_\odot\ \mathrm{yr}^{-1}$, the instability strip does not cover such cases as explained above. This well explains why the maser sources that have such a short periodic variability have not been observed.

Our calculations predict that both the period and luminosity of the pulsationally unstable protostars increase with the accretion

Table 1
Methanol Maser Sources with Periodic Variability

Source	$P_{\rm met}$	$D_{\rm src}$	L_{IRAS}	References	
				P	D
(Galactic Name)	(days)	(kpc)	($10^4\,L_\odot$)		
009.621+0.196	244	5.2	30.0	1	6
012.681−0.182	307	4.5	4.2	2	7
012.889+0.489	29.5	2.34	2.0	3	8
022.357+0.066	179.2	4.6	2.4	4	9
037.550+0.200	237	5.0	4.5	5	9
188.946+0.886	404	2.10	1.2	1	10
196.454−1.677	668	5.28	10.2	2	11
328.237−0.547	220	12.0	117.2	1	9
331.132−0.244	504	4.7	6.2	1	7
338.935−0.062	133	2.9	3.8	1	9
339.622−0.121	201	2.6	1.6	1	9

Notes. Column 1: name of the source; Column 2: variability period; Column 3: distance; Column 4: luminosity estimated with the *IRAS* data; Columns 5 and 6: references of the periods (P) and distances (D).
[a] Assumed on a flat rotation curve with a Galactic circular rotation of the Sun, of 246 km s^{-1} (Bovy et al. 2009), and a solar distance, of 8.4 kpc (e.g., Reid et al. 2009b).
References. (1) Goedhart et al. 2007; (2) Goedhart et al. 2004; (3) Goedhart et al. 2009; (4) Szymczak et al. 2011; (5) Araya et al. 2010; (6) Sanna et al. 2009; (7) Near kinematic distance[a]; (8) Xu et al. 2011; (9) Green & McClure-Griffiths 2011; (10) Reid et al. 2009a; (11) Honma et al. 2007.

rate. We thus predict a positive correlation between the maser periodicity and the stellar luminosity. We fit the unstable models by a single power law and obtain the period–luminosity (P–L) relation (thick line in Figure 2)

$$\log(L/\,L_\odot) = 4.62 + 0.98\log(P/100\,\mathrm{days}), \qquad (1)$$

which is similar to that of the Cepheids ($L \propto P^{4/3}$) and is well used as a cosmic distance ladder (e.g., Tammann et al. 2003; Sandage et al. 2004). The above P–L relation and the instability strip can explain the distribution of the observed parameters in the periodic methanol masers within errors of an order of magnitude. In the Appendix, we show that a similar P–L relation is analytically derived.

The instability strip shown in Figures 1 and 2 is not broad. The duration for which a protostar is in the strip, i.e., the prospective lifetime of each periodic maser source, is only $\sim 10^3$ yr. This actually matches the rarity expected from observations. The number of 6.7 GHz methanol masers observed ever is ∼900 (e.g., Pestalozzi et al. 2005; Caswell et al. 2011; Green et al. 2012), and of those, 56 masers have been monitored for more than a year at intervals shorter than a week or a month (Goedhart et al. 2007, 2009; Araya et al. 2010; Szymczak et al. 2011). About 20% of such sources show the characteristic periodic variabilities (Table 1). Figure 2 might suggest that our models are more applicable to the sources with shorter periods, e.g., $P \lesssim 0.5$ yr, which is only $\simeq$5% of the monitored sources. Since the appearance time of the methanol masers during massive star formation is thought to be $\simeq 3 \times 10^4$ yr (van der Walt 2005), the lifetime of the periodic maser sources should be as short as expected from our calculations.

An uncertainty of the P–L relation arises from possible variations of our stellar evolution tracks. While HO09 study protostellar evolution with spherical accretion, for instance, HYO10 present that the evolution slightly changes with different

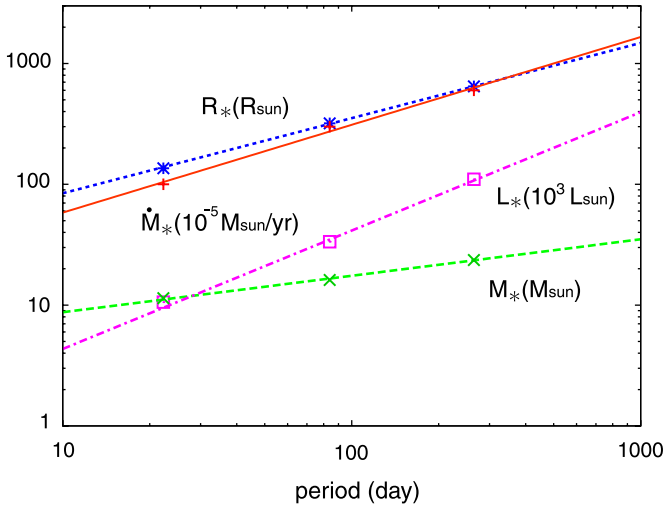

Figure 3. Dependences of the protostellar properties (the stellar radius R_*, luminosity L_*, mass M_*, and accretion rate $\dot{M}_*$) on the period in the stellar-pulsation models. Each line fits the results of the stability analysis (symbols) by a single power-law function (see Equations (1)–(4)).
(A color version of this figure is available in the online journal.)

accretion geometries, e.g., accretion via a geometrically thin disk.[6] We also perform the stability analysis of the case MD3-D-b0.1 in HYO10, whose model has the largest radius among the cases for $\dot{M}_* = 10^{-3}\,M_\odot\,\mathrm{yr}^{-1}$. Figure 2 shows that the protostar also becomes pulsationally unstable in this case, and that the periods are 10 times longer than those with the spherical accretion at the same rate. This effect might explain the observed sources that have longer periods than predicted by the P–L relation (Equation (1)).

4. CONCLUSION AND DISCUSSION

In this Letter, we have shown that the pulsation of massive protostars could explain the periodic variability of the 6.7 GHz maser sources. Our linear stability analysis clearly shows that a rapidly accreting ($\dot{M}_* \gtrsim 10^{-3}\,M_\odot\,\mathrm{yr}^{-1}$) massive protostar becomes pulsationally unstable when the star is bloated before reaching the ZAMS. Typical periods of the pulsation are several 10–100 days, which well explain the observed periodicity. The period depends on the adopted accretion rate, getting longer with the higher rate. On the other hand, protostars with lower $\dot{M}_*$ become unstable but do not produce the periodicity, which could also explain why a periodic variability shorter than 10 days has not been observed. Our stability analysis predicts the P–L relation for the pulsationally unstable protostars, $\log(L/\,L_\odot) = 4.62 + 0.98\log(P/100\,\mathrm{days})$.

Moreover, our stellar evolution models predict that other stellar properties such as the mass, radius, and accretion rate as well as the luminosity should depend on the pulsation period. We show this in Figure 3. Single power-law functions that fit the results are

$$M_* = 17.5\,M_\odot \left(\frac{P}{100\,\mathrm{days}}\right)^{0.30}, \qquad (2)$$

[6] While the "disk accretion" mentioned here assumes the lowest entropy of the accreting gas, the rapid mass accretion could enhance the entropy (e.g., Hosokawa et al. 2011). In this case, the stellar evolution with the spherical accretion would be more realistic even if gas accretes through the disk (see HYO10).

$$R_* = 350\,R_\odot \left(\frac{P}{100\,\mathrm{days}}\right)^{0.62}, \quad (3)$$

$$\text{and } \dot{M}_* = 3.1\times10^{-3}\,M_\odot\,\mathrm{yr}^{-1}\left(\frac{P}{100\,\mathrm{days}}\right)^{0.73}. \quad (4)$$

If the P–L relation (Equation (1)) is confirmed by further observations, we can infer the above quantities with Equations (2)–(4) only from the maser period. As seen in Figure 2, the periods of the observed maser sources are longer than 10 days. Our stellar-pulsation models predict that, in particular to explain the periods longer than 100 days, very rapid mass accretion with $\dot{M}_* \gtrsim 3\times10^{-3}\,M_\odot\,\mathrm{yr}^{-1}$ is required. In this way, we can make a direct diagnosis of the small-scale structure of accreting massive protostars and their vicinities ($\lesssim$ a few AU), which are difficult to see in the optical and infrared bands, by measuring the maser periods.

The stellar pulsation examined above should cause the periodic variation of the stellar luminosity L_*. Although it is still uncertain where the maser emission is excited around protostars, some observations suggest that the maser sources are located on circumstellar disks at $r \sim 10^3$ AU (e.g., Bartkiewicz et al. 2009). The temperature of the circumstellar disk irradiated by the stellar radiation obeys $T_\mathrm{d}(r) \simeq 120\,\mathrm{K}(L_*/3\times10^4\,L_\odot)^{1/4}(r/10^3\,\mathrm{AU})^{-1/2}$, where r is the distance from the protostar. The variation of the stellar luminosity δL_* changes the dust temperature following $\delta T_\mathrm{d}/T_\mathrm{d} \simeq \delta L_*/4L_*$. Since the response of the dust temperature to the irradiating flux variation is so rapid ($\sim$ a few sec), δT_d should synchronize with δL_*. As evaluating δL_* is beyond our linear analysis, we here consider the flux variation of Mira variables that are also excited by the κ-mechanism. Interestingly, SiO maser sources associated with some Mira variables are likely pumped by the stellar radiation and show periodic variations that synchronize with the stellar pulsation (Pardo et al. 2004). With the typical flux variations of $\simeq$3 mag of Mira-type stars (Samus et al. 2009), the amplitude of the variation is estimated as $\delta T_\mathrm{d}/T_\mathrm{d} \simeq 0.3$, which results in $\delta T_\mathrm{d} \simeq 40$ K around $T_\mathrm{d} \simeq 120$ K. Cragg et al. (2005) show that the variations of the dust temperature $\delta T_\mathrm{d} \gtrsim 20$ K could produce the observed amplitudes of the maser variability ($\sim$10–100 Jy). Therefore, the stellar pulsation could produce the flux variations of the observed 6.7 GHz methanol masers.

In the above, we have supposed that the stellar radiation reaches the irradiated disk surface without significant time delays, i.e., the light path from the star to the disk surface is optically thin. This should be valid with the disk accretion, where the density above the disk quickly decreases as the gas falls onto the disk. If outflow is launched from the disk, however, the disk wind would enhance the density above the disk and increase the optical depth. According to a disk wind model by Zhang et al. (2013), the optical depth when the protostar is pulsationally unstable is estimated as $\simeq 5(\dot{M}_*/10^{-3}\,M_\odot\,\mathrm{yr}^{-1})^{0.27}(\bar{\kappa}/3\,\mathrm{cm}^2\,\mathrm{g}^{-1})$, where $\bar{\kappa}$ is the mean opacity of dusts. The diffusion time with this optical depth is $\simeq$30 days, which is shorter than the typical periods of the maser sources. This effect would smear out only variabilities shorter than a few 10 days. Nonetheless, the launching mechanism of the disk wind and the detailed density structure above the disk are still highly uncertain. Some periodic maser sources that have $P \gtrsim 100$ days also show rapid fluctuations of light curves over a few 10 days (G009.621, G022.357, and G338.935). The above estimate of the diffusion time do not explain such rapid changes. Although the variations of these sources might be explained with different models rather than ours (also see below), it would also be possible that the disk wind is weaker and the diffusion time is shorter than evaluated above. Simultaneous monitoring of the maser sources in the infrared band will verify the relation between the periodic variations of the stellar luminosity and the maser variability.

Finally, we compare our pulsation model with alternative models for explaining the periodic variability of the 6.7 GHz methanol maser sources. For instance, van der Walt (2011) proposes that radiation from shocked gas in the colliding binary wind explains both the periodicity and shapes of the light curves of some maser sources. This model supposes a particular condition, the binary system surrounded by an ultracompact H II region ($\sim10^3$ AU), and explains the periodic maser sources for which ultracompact H II regions have been observed (triangles in Figure 2). On the other hand, a number of sources presented in Figure 2 do not show associated H II regions at least at 5 and 8 GHz. Our models could explain these sources, as the protostar becomes pulsationally unstable when the stellar radius is very large and effective temperature is only $T_\mathrm{eff} \simeq 5000$ K, with which the UV luminosity is too low to create a detectable H II region. This suggests that measuring the UV luminosities of massive protostars would be a key for discriminating the models. Further observations at higher frequencies (> a few tens GHz) would detect hypercompact H II regions, which are too small and optically thick to be detected at the lower frequencies. Such observations with higher spatial resolution (e.g., with ALMA) are sure to advance our understanding of the enigmatic periodic variability of the maser sources.

We thank Kazuyuki Omukai, Munetake Momose, Yoshinori Yonekura, Kenta Fujisawa, Mareki Honma, Yichen Zhang, Takashi Nakamura, Yudai Suwa, and Daisuke Nakauchi for their fruitful discussions. This work is supported in part by the Grants-in-Aid by the Ministry of Education, Culture, and Science of Japan (23·838 K.I. and 24·6525 K.M.) and by the Yamaguchi University project entitled "The East-Asian VLBI Network and the Circulation of Matter in the Universe."

APPENDIX

ANALYTIC DERIVATION OF THE P–L RELATION

In this Appendix, we analytically derive a P–L relation similar to Equation (1) by considering the protostellar evolution. Stahler et al. (1986, hereafter SPS86) show that the evolution of an accreting protostar is well understood with the balance between the following two timescales: the accretion timescale $t_\mathrm{acc} = M_*/\dot{M}_*$ and the KH timescale $t_\mathrm{KH} = GM_*^2/L_*R_*$. As seen in Figure 1, the protostar gradually expands in the early stage with $t_\mathrm{acc} < t_\mathrm{KH}$ and turns to contract in the later stage with $t_\mathrm{acc} > t_\mathrm{KH}$. The turnaround of the radius occurs when $t_\mathrm{acc} \simeq t_\mathrm{KH}$ (also see HO09 and HYO10). According to our linear stability analysis, the protostar becomes unstable at the epoch of the maximum radius, i.e., $t_\mathrm{acc} \simeq t_\mathrm{KH}$ (see star symbols in Figure 1).

SPS86 also show that the stellar expansion in the early evolutionary stage is well described as $R_* \propto {M_*}^{0.27}\,{\dot{M}_*}^{0.41}$. With Kramers' law $\kappa \propto \rho T^{-7/2}$, which approximates the dependences of opacity in the stellar interior in this early stage, the stellar luminosity generally obeys $L_* \propto {M_*}^{11/2}{R_*}^{-1/2}$ (e.g., Cox & Giuli 1968). Using these relations, we can express the luminosity of the unstable protostar (i.e., $t_\mathrm{acc} \simeq t_\mathrm{KH}$) as a function of the pulsation period $P(\propto R_*^{3/2}M_*^{1/2})$ and obtain the P–L relation $L_* \propto P^{1.2}$.

REFERENCES

Appenzeller, I. 1970, A&A, 5, 355
Araya, E. D., Hofner, P., Goss, W. M., et al. 2010, ApJL, 717, L133
Bartkiewicz, A., Szymczak, M., van Langevelde, H. J., Richards, A. M. S., & Pihlström, Y. M. 2009, A&A, 502, 155
Beltrán, M. T., Cesaroni, R., Codella, C., et al. 2006, Natur, 443, 427
Bovy, J., Hogg, D. W., & Rix, H.-W. 2009, ApJ, 704, 1704
Casoli, F., Combes, F., Dupraz, C., Gerin, M., & Boulanger, F. 1986, A&A, 169, 281
Caswell, J. L., Fuller, G. A., Green, J. A., et al. 2011, MNRAS, 417, 1964
Cox, J. P. 1980, Theory of Stellar Pulsation (Princeton, NJ: Princeton Univ. Press)
Cox, J. P., & Giuli, R. T. 1968, Principles of Stellar Structure (New York: Gordon and Breach)
Cragg, D. M., Sobolev, A. M., & Godfrey, P. D. 2005, MNRAS, 360, 533
Goedhart, S., Gaylard, M. J., & van der Walt, D. J. 2004, MNRAS, 355, 553
Goedhart, S., Gaylard, M. J., & van der Walt, D. J. 2007, in IAU Symp. 242, Astrophysical Masers and their Environments, ed. J. M. Chapman & W. A. Baan (Cambridge: Cambridge Univ. Press), 97
Goedhart, S., Langa, M. C., Gaylard, M. J., & van der Walt, D. J. 2009, MNRAS, 398, 995
Green, J. A., Caswell, J. L., Fuller, G. A., et al. 2012, MNRAS, 420, 3108
Green, J. A., & McClure-Griffiths, N. M. 2011, MNRAS, 417, 2500
Guzmán, A. E., Garay, G., Brooks, K. J., & Voronkov, M. A. 2012, ApJ, 753, 51
Harries, T. J., Hilditch, R. W., & Howarth, I. D. 2003, MNRAS, 339, 157
Hilditch, R. W., Howarth, I. D., & Harries, T. J. 2005, MNRAS, 357, 304
Honma, M., Bushimata, T., Choi, Y. K., et al. 2007, PASJ, 59, 889
Hosokawa, T., Offner, S. S. R., & Krumholz, M. R. 2011, ApJ, 738, 140
Hosokawa, T., & Omukai, K. 2009, ApJ, 691, 823 (HO09)
Hosokawa, T., Yorke, H. W., & Omukai, K. 2010, ApJ, 721, 478 (HYO10)
Inayoshi, K., Hosokawa, T., & Omukai, K. 2013, arXiv:1302.6065
Krumholz, M. R., Klein, R. I., McKee, C. F., Offner, S. S. R., & Cunningham, A. J. 2009, Sci, 323, 754
Lada, C. J., & Lada, E. A. 2003, ARA&A, 41, 57
McKee, C. F., & Tan, J. C. 2003, ApJ, 585, 850
Norris, R. P., Whiteoak, J. B., Caswell, J. L., Wieringa, M. H., & Gough, R. G. 1993, ApJ, 412, 222
Osorio, M., Lizano, S., & D'Alessio, P. 1999, ApJ, 525, 808
Pardo, J. R., Alcolea, J., Bujarrabal, V., et al. 2004, A&A, 424, 145
Pestalozzi, M. R., Minier, V., & Booth, R. S. 2005, A&A, 432, 737
Reid, M. J., Menten, K. M., Brunthaler, A., et al. 2009a, ApJ, 693, 397
Reid, M. J., Menten, K. M., Zheng, X. W., et al. 2009b, ApJ, 700, 137
Samus, N. N., et al. 2009, yCat, 1, 2025
Sandage, A., Tammann, G. A., & Reindl, B. 2004, A&A, 424, 43
Sanna, A., Moscadelli, L., Cesaroni, R., et al. 2010, A&A, 517, A78
Sanna, A., Reid, M. J., Moscadelli, L., et al. 2009, ApJ, 706, 464
Stahler, S. W., Palla, F., & Salpeter, E. E. 1986, ApJ, 302, 590 (SPS86)
Szymczak, M., Wolak, P., Bartkiewicz, A., & van Langevelde, H. J. 2011, A&A, 531, L3
Tammann, G. A., Sandage, A., & Reindl, B. 2003, A&A, 404, 423
Unno, W., Osaki, Y., Ando, H., Saio, H., & Shibahashi, H. 1989, Nonradial Oscillations of Stars (2nd ed.; Tokyo: Univ. Tokyo Press)
Urquhart, J. S., Busfield, A. L., Hoare, M. G., et al. 2007, A&A, 461, 11
van der Walt, D. J. 2011, AJ, 141, 152
van der Walt, J. 2005, MNRAS, 360, 153
Walsh, A. J., Burton, M. G., Hyland, A. R., & Robinson, G. 1998, MNRAS, 301, 640
Xu, Y., Moscadelli, L., Reid, M. J., et al. 2011, ApJ, 733, 25
Yoon, S.-C., & Cantiello, M. 2010, ApJL, 717, L62
Zhang, Q., Hunter, T. R., Brand, J., et al. 2005, ApJ, 625, 864
Zhang, Y., Tan, J. C., & McKee, C. F. 2013, ApJ, 766, 86